Applied Catalysis B: Environmental 259 (2019) 117958

Contents lists available at ScienceDirect

Applied Catalysis B: Environmental

journal homepage: www.elsevier.com/locate/apcatb

Utilization of photochemical circulation between NO_3^- and NO_2^- in water to degrade photoinert dimethyl phthalate: Influence of organic media and mechanism study

Lijie Xu[a], Yang Sun[a], Lu Gan[b,*], Jiangang Han[a], Ping Wang[a], Lei Yu[a], Xiang Mei[a], Wei Li[a], Baoling Lyu[a], Chun Pei[c], Wei Chu[d,*]

[a] College of Biology and the Environment, Nanjing Forestry University, Nanjing, 210037, Jiangsu, People's Republic of China
[b] College of Materials Science and Engineering, Nanjing Forestry University, Nanjing, 210037, Jiangsu, People's Republic of China
[c] Guangdong Province Key Laboratory of Durability for Marine Civil Engineering, School of Civil Engineering, Shenzhen University, Shenzhen, Guangdong 518060, People's Republic of China
[d] Department of Civil and Environmental Engineering, The Hong Kong Polytechnic University, Hung Hom, Kowloon, Hong Kong

ARTICLE INFO

Keywords:
Nitrate
Nitrite
Dimethyl phthalate
Photochemical
Cycling

ABSTRACT

Photoconversion of NO_3^-/NO_2^- at wastewater relevant concentrations as an advanced oxidation approach to degrade dimethyl pthalate (DMP), a relatively photoinert endocrine disruptor, were examined. Three different wavelengths (350 nm, 300 nm, 254 nm) were involved. The influence of NO_3^- or NO_2^- was found to be wavelength-dependent. The 254 nm UV light could decompose DMP efficiently, but photolysis of DMP was slow at $\lambda = 300$ nm and noneffective at $\lambda = 350$ nm, which could be catalyzed by the presence of NO_3^- or NO_2^-. Both $^{\cdot}OH$ and $O_2^{\cdot -}$ were detected, while $^{\cdot}OH$ was identified as the primary contributor to DMP decomposition. NO_2^- plays a dual role as both a source and sink of $^{\cdot}OH$, depending on the relative abundance between NO_2^- and DMP. NO_3^- was more efficient than NO_2^- for treating low-level DMP. However, higher organic content could effectively inhibit the quenching role of NO_2^-, making NO_2^- more efficient for catalyzing DMP decomposition. For irradiation at $\lambda = 350$ nm, NO_3^- was completely ineffective, while self regeneration of NO_2^- enabled $\Delta[NO_2^-]:\Delta[^{\cdot}OH] << 1$. For irradiation at $\lambda = 300$ nm, cycling between NO_2^- and NO_3^- occurred, and the transformation from NO_2^- to NO_3^- proceeded much faster. Complete decomposition of DMP at concentrations higher than those of NO_2^- or NO_3^- was observed, and mineralization was also achieved. Based on the identification of the intermediates, $^{\cdot}OH$ addition to the aromatic ring and hydrogen atom abstraction by $^{\cdot}OH$ were the dominant pathways, while nitration products were detected at low levels.

1. Introduction

Nitrate and nitrite ions are ubiquitous in natural water bodies, and are also important products of the activated sludge wastewater treatment processes (e.g., nitrification or partial nitrification), with concentrations ranging from several to dozens of mg/L or even higher depending on the influent quality and treatment technology. NO_3^- and NO_2^- are always regarded as the nutrients that must be removed with no effective utilization. Previous studies have reported on the photochemical activities of NO_3^- and NO_2^- that could produce multiple radicals and reactive oxygen (e.g., $^{\cdot}OH$, $O^{\cdot -}$, $O(^3P)$) [1]. The absorption spectra of NO_3^- and NO_2^- are dominated by the $\pi \rightarrow \pi^*$ transitions at 200 nm and 205 nm, respectively. NO_3^- and NO_2^- also display $n \rightarrow \pi^*$ absorption bands at 310 nm and 360 nm, respectively, that overlap with the solar spectrum reaching the Earth's surface [1].

Indirect transformation of some persistent organic pollutants in sunlit surface waters by NO_3^-/NO_2^--induced reactive transient species has been reported [2,3]. However, utilizing the photoactivity of NO_3^-/NO_2^- in natural water to degrade organic micropollutants will at most serve as a feasible self-purification process that is limited by its low efficiency due to the very low concentration of NO_3^-/NO_2^- in natural water and the hysteretic nature since the pollutants have already been discharged to the natural environment. Applying the photochemical reactions of NO_3^-/NO_2^- at relatively high concentrations as an advanced oxidation technology (AOT) to replace the use of H_2O_2 that has relatively low molar absorption coefficient may provide a cost-effective approach to control the release of micropollutants during conventional wastewater treatment processes if a proper arrangement is allowed for

* Corresponding authors.
E-mail addresses: ganlu@njfu.edu.cn (L. Gan), cewchu@connect.poly.hk (W. Chu).

https://doi.org/10.1016/j.apcatb.2019.117958
Received 27 March 2019; Received in revised form 1 July 2019; Accepted 12 July 2019
Available online 10 August 2019
0926-3373/

taking full advantage of the in situ produced NO_3^-/NO_2^-. Compared to traditional photocatalysis using various semiconductors, metallic (e.g., bismuth catalysts [4–7]) or nonmetallic (e.g., C_3N_4 [8]), NO_3^-/NO_2^--based homogeneous photocatalytic process also has the advantage of dispensing with catalyst separation. The high concentration of NO_3^-/NO_2^- can be easily removed by denitrification process.

Although NO_3^-/NO_2^- photolysis mechanisms have been the subject of considerable controversy in the literature, the use of NO_3^-/NO_2^--based AOT to treat As(III) and organic pollutants has achieved some promising results [9–15]. NO_3^- and NO_2^- were found to improve the decomposition of many organic contaminants, such as herbicides [11], endocrine disruptors [16], caffeine [17], antibiotics [18], and drugs [19]. In particular, a previous study (2012) found that nitrified wastewater containing a high amount of NO_3^- can provide advanced oxidation in the UV disinfection process, significantly decreasing the effluent trace organic pollutants [20]. Additionally, the concentration of $^{\cdot}OH$ produced by 5 mg/L-N of nitrate was comparable to that produced by the addition of 10 mg/L H_2O_2 [20]. However, only the promoting effects were evaluated in these studies with no analysis of the mechanisms involved in the cycling of NO_3^-/NO_2^-. One systematic study (Kim et al. 2014) reported on the effective oxidation of As(III) to As(V) by the photochemical circulation between NO_3^- and NO_2^-, with $^{\cdot}OH$, $NO_2^{\cdot}$, and $O_2^{\cdot-}$ considered as the reactive transient species, and NO_2^- was found to be more efficient for As(III) oxidation [10]. Nonetheless, even though the photochemical transformation between NO_3^- and NO_2^- may be different when mediated by metal ions or organic compounds, hardly any studies have considered the influence of different media on NO_3^-/NO_2^- photoconversion.

In this study, UV photolysis of NO_3^- and NO_2^- at relatively high concentrations (wastewater relevant) was investigated as an AOT for the degradation of the endocrine disruptor dimethyl phthalate (DMP) as a selected contaminant of emerging concern. DMP was selected mainly because of its heavy use as a plasticizer and its relatively high water solubility (4000 mg/L at 25 °C [21]) that increases its concentration in water. DMP is relatively stable in the natural environment with long hydrolysis half-time and low photon yield [22]. The kinetics of DMP degradation and the accompanying NO_3^-/NO_2^- conversion were investigated in detail. The role of NO_3^-/NO_2^- in catalyzing DMP degradation was analyzed under different UV conditions. The degradation mechanisms were studied based on the identification of reactive oxygen species (ROS) and DMP degradation intermediates.

2. Experimental section

2.1. Chemicals

Chemicals used in this study included: DMP (> 99%, TCI), $NaNO_3$ (≥99.999%, Fluka), $NaNO_2$ (≥99.999%, Aldrich), coumarin (> 99%, Energy Chemical), 7-hydroxycoumarin (> 99%, Aldrich), and 5,5-Dimethyl-1-pyrroline N-oxide (DMPO) (≥97%, Macklin). Reagents included methanol (HPLC grade, Tedia) and tert butyl alcohol (TBA) (≥99.5%, Aldrich). Chemicals and reagents were all used as received without further purification. Deionized-distilled water prepared from a Millipore Waters Milli-Q water purification system was used exclusively.

2.2. Photoreactions

The photochemical reactions were all carried out under air-equilibrated condition without artificial aeration. Experiments were conducted in a tailor-made photo-reactor and a coolant thermostat was used to provide water bath temperature control (Fig. S1). Solution temperature was kept at 22 ± 1 °C. UV mercury lamps with three different wavelengths (254 nm, 300 nm, 350 nm) were purchased from Rayonet®.org and the emission spectra were given in Fig. S2. Ten lamps were used for each wavelength and the incident photon intensities were 1.71×10^{-5} Einstein L^{-1} s^{-1} (254 nm), 6.92×10^{-6} Einstein L^{-1} s^{-1} (300 nm), and 5.2×10^{-5} Einstein L^{-1} s^{-1} (350 nm) determined by chemical actinometer, potassium ferrioxalate. Quartz beakers with magnetic stirring were used throughout and the initial solution volume was 250 mL. Solution pH was not adjusted or buffered with initial value of 6.2 ± 0.2.

2.3. Analytical methods

DMP concentration was determined by high performance liquid chromatography (HPLC) (Dionex Ultimate 3000). A mobile phase of methanol/0.1% phosphoric acid water solution (60/40, vol/vol) was employed. Quantitative analyses of NO_3^- and NO_2^- were conducted using ion chromatography (IC, Dionex ICS-900) equipped with a Dionex Ionpac AS15 (4 × 250 mm) column, AERS 500 anion suppressor and a conductivity detector. The eluent was 38 mM KOH water solution and the flow rate was 1.2 mL min^{-1}. The UV absorption spectra were scanned by Perkin Elmer Lambda 25 UV/vis spectrophotometer. Intermediates identification was performed using Agilent 6540 Q-TOF LC/MS. The mobile phase was obtained by mixing different ratios of acetonitrile and water at the flow rate of 0.2 mL min^{-1} with the gradient programme shown in Fig. S3. The concentration of H_2O_2 was determined by measuring the absorbance of titanium peroxide (TiO_2^{2+}) using a spectrophotometer at 405 nm [23].

Coumarin (0.1 or 1 mM) was applied as a probe for $^{\cdot}OH$ quantification (Scheme S1) [24]. Formation of 7-hydroxycoumarin was measured by fluorescence spectrometry (PerkinElmer LS 55). Fluorescence emission was detected at 456 nm under excitation at 332 nm. Total organic carbon (TOC) was quantified by Analytik Jena multi N/C 3100 TOC. Total nitrogen (TN) was determined by measuring the absorbance at 220 nm and 275 nm after digestion at 122 °C using $K_2S_2O_8$ as the oxidant [25]. Electron spin resonance (ESR) signals were detected by Bruker EMX-10/12 equipment with X-band field sweep. The settings were: center field = 3480 G, sweep width = 200 G, micro frequency = 9.736 GHz, power = 19.92 mW. DMPO (70 mM) was used as the trapping agent, and all samples were tested after 30 min reaction. The molar ratio coefficients of involved compounds were calculated based on Beer-Lambert Law (Test S1).

3. Results and discussion

3.1. Effect of UV wavelength

Reactions that should be involved in the UV/DMP/NO_x^- (x = 2, 3) system are listed in Table 1. The UV absorption spectra of NO_3^- and NO_2^- were recorded in Fig. S4. Since the strongest n→π* absorption of NO_3^- and NO_2^- was obtained at 302 nm (ε = 7.01 M^{-1} cm^{-1}) and 355 nm (ε = 22.66 M^{-1} cm^{-1}), respectively, their photochemical activities were assumed to be wavelength-dependent. Hence, photodegradation of DMP with and without the addition of NO_x^- was investigated at the two most relevant wavelengths (300 nm and 350 nm), and another UV wavelength (254 nm) most widely adopted in wastewater treatment was also investigated (see Fig. 1).

The effect induced by the presence of 0.5 mM NO_x^- (NO_2^- or NO_3^-) was found to depend strongly on the incident light. At λ = 350 nm, DMP was inert when irradiated by UV alone due to its transparency at λ > 300 nm (Fig. S5). Removal of approximately 28% DMP was observed in the presence of NO_2^- and hardly any difference was observed after adding NO_3^-, mainly due to the strong light absorption of NO_2^- at 350 nm (ε_{350} = 22.22 M^{-1} cm^{-1}) and very weak light absorption of NO_3^- (ε_{350} = 0.02 M^{-1} cm^{-1}) at this band. DMP degradation under UV_{350nm} irradiation was thus ascribed completely to the photosensitizing effect of NO_2^-. At λ = 300 nm, 20% of DMP was decomposed by direct photolysis. It should be noted that generally all the groups of phthalic acid dialkyl esters showed relatively low quantum yields by photolysis and DMP with the shortest chain

Table 1
Reactions that should be involved in UV/NO_3^-/DMP or UV/NO_2^-/DMP systems.

	Reactions	*k*	Ref
A1	$NO_2^- + h\nu \rightarrow NO_2^{\cdot}$*		[1]
A2	$NO_2^{\cdot}$* → NO˙ + O˙-		[1]
A3	$O^{\cdot-} + H_2O \rightarrow {}^{\cdot}OH + OH^-$	$1.7 \times 10^6\ M^{-1}s^{-1}$	[1]
A4	NO˙ + ˙OH → HNO_2 (diffusion control)	$1 \times 10^{10}\ M^{-1}s^{-1}$	[1]
A5	$NO_2^- + {}^{\cdot}OH \rightarrow NO_2^{\cdot} + OH^-$ (diffusion control)	$1 \times 10^{10}\ M^{-1}s^{-1}$	[1]
A6	NO˙ + $NO_2^{\cdot} \rightarrow N_2O_3$	$1.1 \times 10^9\ M^{-1}s^{-1}$	[1]
A7	$N_2O_3 + H_2O \rightarrow 2H^+ + 2NO_2^-$	$5.3 \times 10^2\ s^{-1}$	[1]
A8	$2NO_2^{\cdot} \rightarrow N_2O_4$	$4.5 \times 10^8\ M^{-1}s^{-1}$	[1]
A9	$N_2O_4 + H_2O \rightarrow NO_2^- + NO_3^- + H^+$	$1 \times 10^3\ s^{-1}$	[1]
A10	NO_2^{-}* → $NO_2^{\cdot}$ + e_{aq}-		[31]
A11	$e_{aq}^- + O_2 \rightarrow O_2^{\cdot-}$	$1.9 \times 10^{10}\ M^{-1}s^{-1}$	[30]
A12	$2NO^{\cdot} + O_2 \rightarrow 2NO_2^{\cdot}$		[31]
A13	$NO^{\cdot} + HO_2^{\cdot} \rightarrow NO_2^{\cdot} + {}^{\cdot}OH$		
A14	$HNO_2 + h\nu \rightarrow NO^{\cdot} + {}^{\cdot}OH$		[31]
A15	$NO_2^{\cdot} + O_2^{\cdot-} \rightarrow O_2 + NO_2^-$	$1 \times 10^8\ M^{-1}s^{-1}$	[1]
A16	$NO^{\cdot} + O_2^{\cdot-} \rightarrow ONOO^-$		[1]
B1	DMP + ˙OH → primary products	$2.67 \times 10^9\ M^{-1}s^{-1}$	[27]
B2	DMP + $O_2 \xrightarrow{254nm}$ (DMP**O_2) → products + $O_2^{\cdot-}$		
B3	$O_2^{\cdot-} + H^+ \rightarrow HO_2^{\cdot}$ (pKa = 4.8)		[28]
B4	$HO_2^{\cdot} + O_2^{\cdot-} + H^+ \rightarrow H_2O_2 + O_2$	$9.7 \times 10^7\ M^{-1}s^{-1}$	[28]
B5	$HO_2^{\cdot} + HO_2^{\cdot} \rightarrow H_2O_2 + O_2$	$8.3 \times 10^5\ M^{-1}s^{-1}$	[28]
B6	$H_2O_2 \xrightarrow{254nm}$ 2˙OH		[29]
C1	$NO_3^- + h\nu \rightarrow NO_3^{\cdot}$*		[1]
C2	NO_3^-* → $NO_2^{\cdot}$ + $O(^3P)$		[1]
C3	NO_3^-* → $NO_2^{\cdot}$ + O˙- $\xrightarrow{H_2O}$ $NO_2^{\cdot}$ + ˙OH + OH-		[1]
C4	$NO_2^{\cdot} + {}^{\cdot}OH \rightarrow HO_2NO$	$1.3 \times 10^9\ M^{-1}s^{-1}$	[30]
C5	$HO_2NO \rightarrow NO_3^- + H^+$ (pH < 7)	$1.4\ s^{-1}$	[1]
D1	H-Ar-H + ˙OH → H-Ar˙ (H)-OH		
D2	H-Ar˙ (H)-OH + O_2 → H-Ar-OH + $HO_2^{\cdot}$		

exhibited the highest stability [22,26]. The quantum yield of DMP decomposition under UV irradiation at 300 nm ($\Phi_{300,\ DMP}$) was 0.249% (detailed calculation is provided in Test S2). Both NO_2^- and NO_3^- improved DMP degradation at 300 nm. However, although NO_2^- (ε_{300} = 9.08 $M^{-1}\,cm^{-1}$) showed slightly higher light absorption than NO_3^- (ε_{300} = 6.97 $M^{-1}\,cm^{-1}$), the presence of NO_3^- accelerated DMP degradation more significantly. This was different from the results observed in metal ion mediated conditions, where NO_2^- was found to be more effective for As(III) oxidation [10]. At λ = 300 nm, larger quantum yield of NO_2^- on the basis of ˙OH generation (reaction A1-A3) was reported (Φ_{308} = 6.9 ± 0.9%) compared to NO_3^- (Φ_{308} = 1.7 ± 0.3%) (reaction C1,C3) [1], indicating the stronger theoretical capability of NO_2^- to produce ˙OH. Therefore, the observed smaller improvement induced by NO_2^- may be related to a possible inhibition effect (discussed below). At λ = 254 nm, the quantum yield for DMP direct photolysis was $\Phi_{254,\ DMP}$ = 0.056% (Test S2), which was lower than $\Phi_{300,\ DMP}$. By contrast, the relatively stronger light absorption of DMP at 254 nm (ε_{254} = 1370 $M^{-1}\,cm^{-1}$ vs. ε_{300} = 30 $M^{-1}\,cm^{-1}$) led to its complete degradation within 10 h (Fig. 1). It was noted that NO_2^- decreased the DMP degradation at 254 nm while NO_3^- showed moderate enhancement. The quantum yields of ˙OH formation during photolysis of NO_2^- (Φ_{254} = 4.6%) and NO_3^- (Φ_{254} = 9%) are reported to be of the same order [1], and additionally, NO_2^- absorbs more light at 254 nm (ε_{254} = 11.74 $M^{-1}\,cm^{-1}$) than NO_3^- (ε_{254} = 3.33 $M^{-1}\,cm^{-1}$). Hence, NO_2^- should have a comparable capability as NO_3^- to produce ˙OH, and an inhibition mechanism was probably also involved for irradiation at 254 nm.

3.2. Effect of nitrite and nitrate dosage

As discussed in 3.1, NO_2^- and NO_3^- showed different influence on DMP degradation, thus various initial concentrations of NO_x^- were applied to further investigate the effects. Since NO_3^- hardly absorbs light at 350 nm, only different $[NO_2^-]_0$ was examined (Fig. S6). Although the presence of NO_2^- could induce DMP degradation at 350 nm, further increase of $[NO_2^-]_0$ exhibited little influence. Hence, a dual role of NO_2^- in producing ROS and consuming ROS should be involved.

Figs. 2 and 3 show the variation profiles of $[DMP]/[DMP]_0$ at different $[NO_x^-]_0$ at λ = 300 nm and 254 nm, respectively. Inset figures show the removal (%) at different NO_x^- levels. For both UV conditions, DMP degradation was gradually accelerated by the increase of $[NO_3^-]_0$ (Figs. 2b and 3 b), suggesting the role of NO_3^- as the precursor of reactive oxidants. Based on reactions C1-C3, the dominant pathway of excited NO_3^- is the production of $O^{\cdot-}$ ($\Phi_{305,\ \dot{O}H}$ = 0.92 ± 0.4% vs. $\Phi_{305,O}$ = 0.11 ± 0.3%) [27], which rapidly reacts with water to form

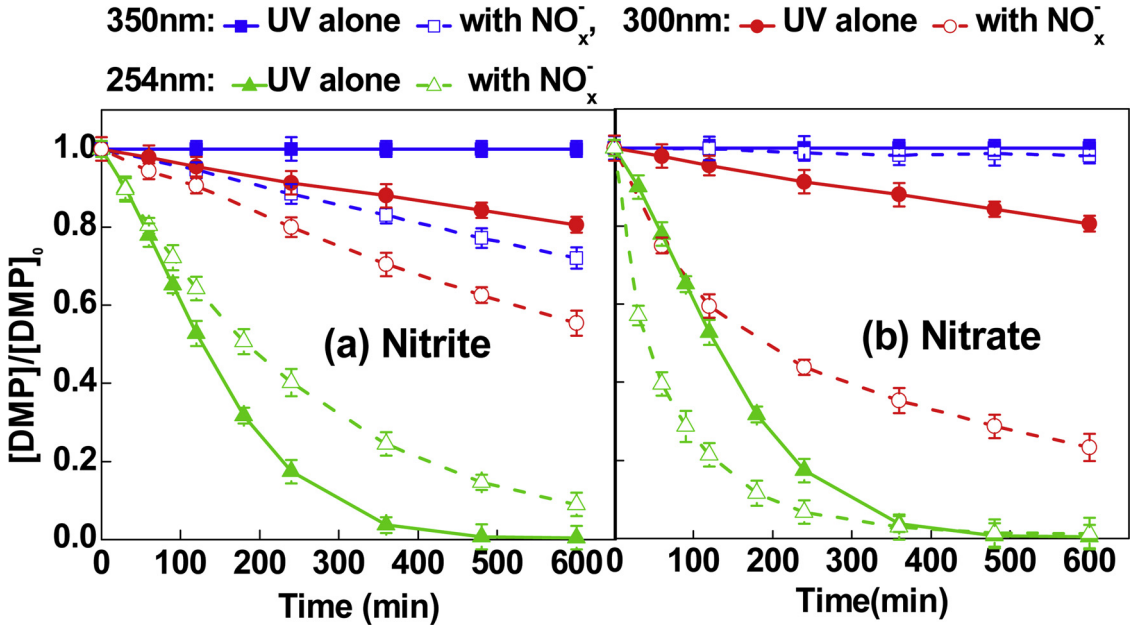

Fig. 1. Effects of nitrite (a) and nitrate (b) on DMP degradation under the UV irradiation at different wavelengths ($[DMP]_0$ = 0.01 mM, $[NO_x^-]_0$ = 0.5 mM, solution volume = 250 mL, pH_0 = 6.2 ± 0.2).

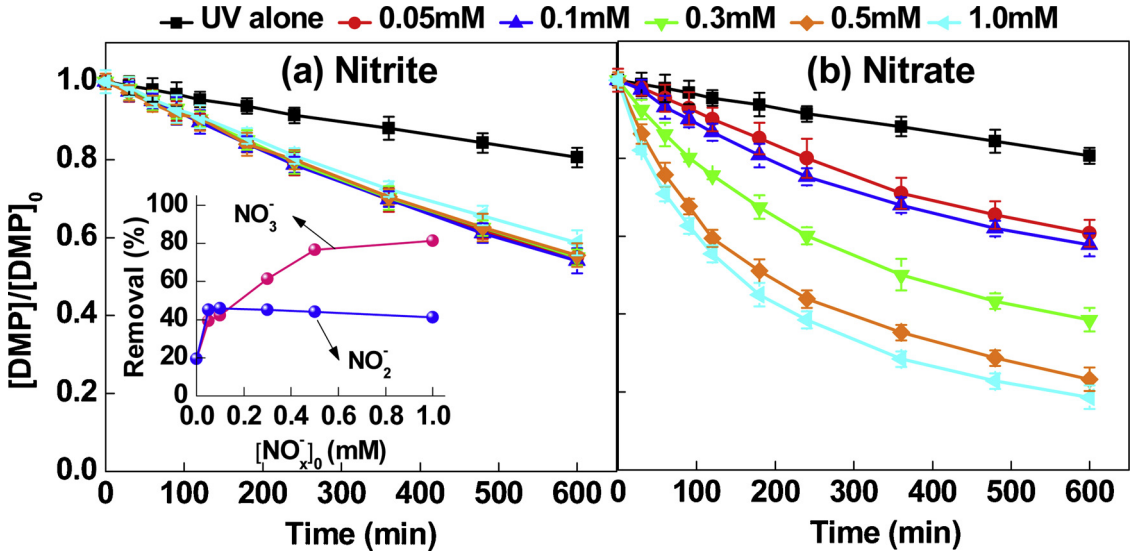

Fig. 2. Effects of initial concentrations of nitrite or nitrate ions on DMP degradation under the irradiation of 300 nm UV light; the inset figure shows DMP removal (%) at different NO_x^- levels ($[DMP]_0$ = 0.01 mM, solution volume = 250 mL, pH_0 = 6.2 ± 0.2).

˙OH. From the inset, it is also found that the rate of removal tended to plateau with higher $[NO_3^-]_0$ due to the scavenging of ˙OH arising from the photoproducts of NO_3^-, in which NO_2˙ (reactions C3 and C4) was proposed to play the major role [20].

At λ = 300 nm (Fig. 2a), NO_2^- was more efficient than NO_3^- in improving DMP degradation at low NO_x^- concentrations (e.g., 0.05 mM), as can be more clearly observed in the inset figure. However, the overall removal rate remained almost unchanged when $[NO_2^-]_0$ was further increased to 1.0 mM, indicating a stable level of available ROS responsible for DMP decomposition even though $[NO_2^-]_0$ increased. The most likely explanation was the self scavenging effect for ˙OH induced by NO_2^- and NO˙ (reactions A4 and A5). Since NO_2^- reacts faster with ˙OH (reaction A5, $k = 1 \times 10^{10}$ $M^{-1}s^{-1}$) than DMP ($k = 2.67 \times 10^9$ $M^{-1}s^{-1}$ [28]), NO_2^- most likely played a dual role in the photoconversion process and greater competition for ˙OH occurred at higher $[NO_2^-]_0$. As reported by Keen et al. (2012) [20], ˙OH production would quickly reach a high level for a nitrite concentration of *ca.* 0.1 mg/L-N and additional nitrite acted as ˙OH scavenger, while the production of ˙OH by nitrate photolysis increased more gently with nitrate concentration, in accordance with the results in the present study.

In particular, at λ = 254 nm (Fig. 3a), the addition of NO_2^- even hampered the photolysis of DMP and the inhibition effect became more pronounced with increasing $[NO_2^-]_0$. The photon competition effect may be excluded due to the dominant advantage of DMP in light absorption compared with NO_2^- ($\varepsilon_{254,\ DMP}$ = 1370 M^{-1} cm^{-1} vs. $\varepsilon_{254,\ NO2-}$ = 11.74 M^{-1} cm^{-1}). The origin of this effect was discussed below in detail.

3.3. Analysis of reactive oxygen species

3.3.1. 254 nm UV condition

In order to unveil the species of ROS and the influence of organic medium on ROS production, ESR analysis was conducted. Fig. 4a shows

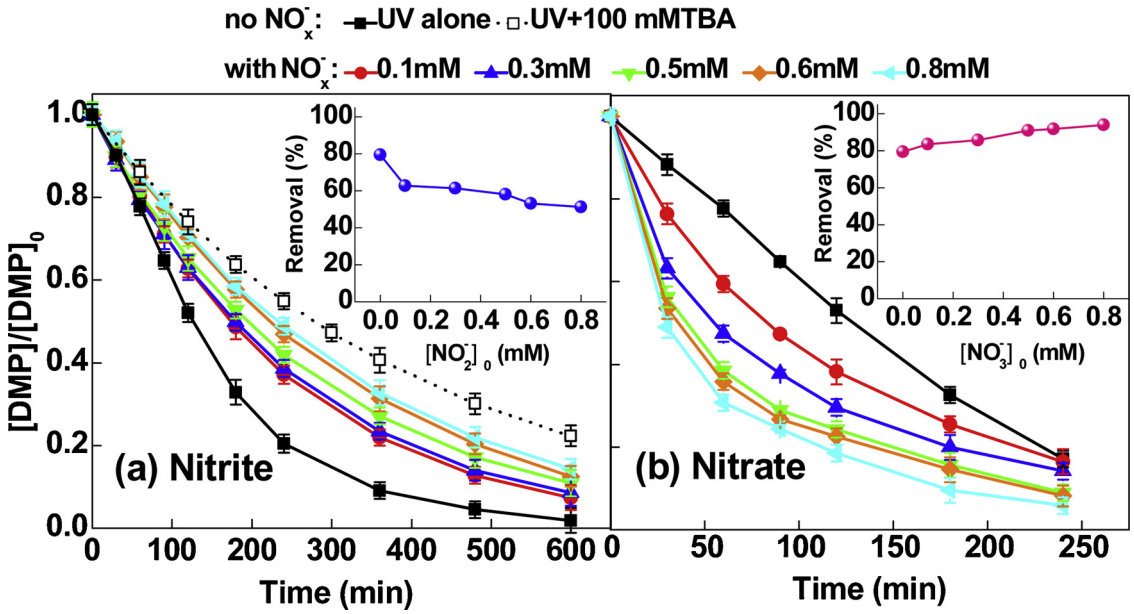

Fig. 3. Effects of initial concentrations of nitrite or nitrate ions on DMP degradation under the irradiation of 254 nm UV light; the inset figures show DMP removal (%) at different NO_x^- levels ($[DMP]_0$ = 0.01 mM, pH_0 = 6.2 ± 0.2).

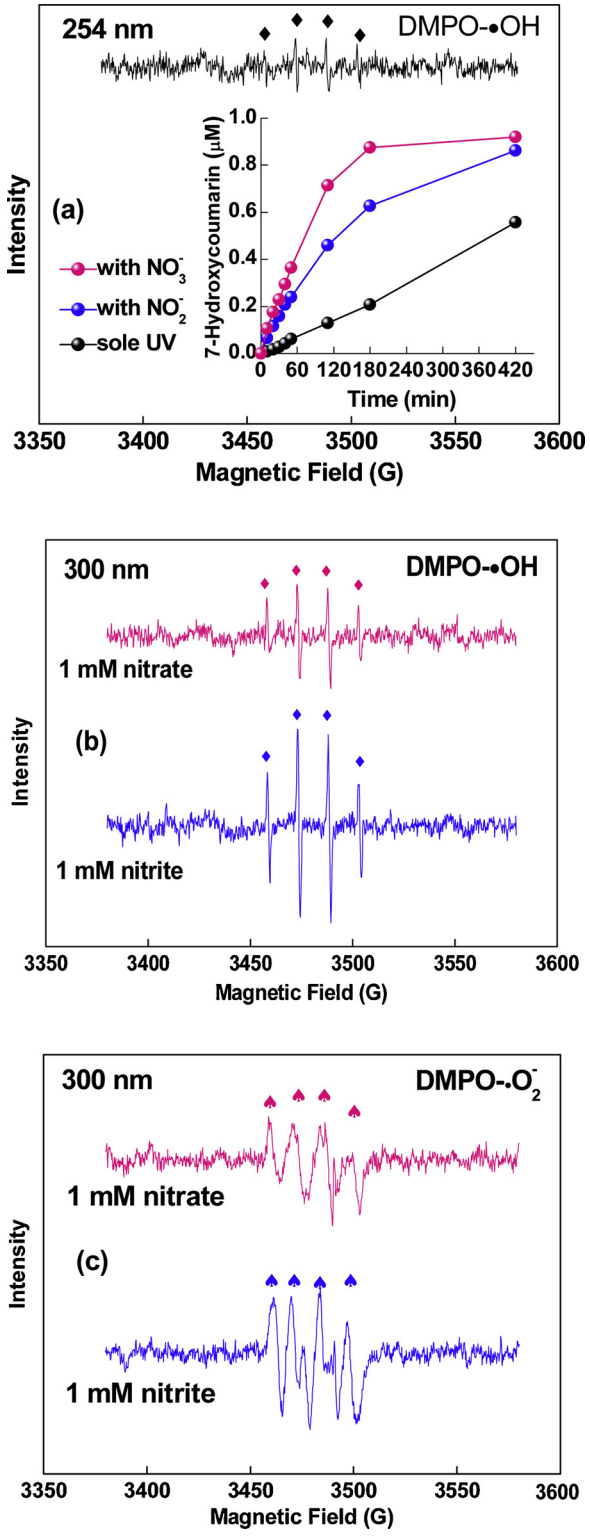

Fig. 4. (a) ESR signal of DMPO spin trapping adducts produced by direct UV-254 nm irradiation without NO_x^- addition; the inset figure shows the formation of 7-hydroxycoumarin with and without NO_x^- addition, (b) ESR signal of DMPO-$^{\cdot}$OH (in water) adduct produced by NO_x^- conversion under UV-300 nm irradiation, (c) ESR signal of DMPO-$^{\cdot}O_2^-$ (in methanol) adduct produced by NO_x^- conversion under UV-300 nm irradiation (conditions: $[DMPO]_0$ = 70 mM, $[DMP]_0$ = 0.01 mM, photon intensity 1.71 × 10^{-5} Einstein L^{-1} s^{-1}, [coumarin] = 0.1 mM, $[NO_x^-]_0$ = 1 mM).

a weak signal exhibiting the characteristic 4-fold peak of DMPO-$^{\cdot}$OH during DMP photolysis at λ = 254 nm, indicating the presence of $^{\cdot}$OH even without NO_x^- addition. The mechanism proposed by Ryu et al. (2013) may explain the origin of $^{\cdot}$OH [29]. Superoxide radical ($O_2^{\cdot -}$) may be formed from dissolved oxygen by accepting an electron from excited DMP molecules (reaction B2). H_2O_2 may form through reactions B3-B5, and then undergoes photo-decomposition at λ = 254 nm to provide $^{\cdot}$OH (B6) [30]. Fig. S7 shows the accumulation of H_2O_2 measured in solution. No H_2O_2 could be detected in pure water, while more H_2O_2 was produced with higher concentrations of DMP, providing strong support for the above hypothesis. The kinetics of DMP decomposition without NO_x- showed a clear lag phase initially (Fig. 3a) due to the gradual formation of neutral $HO_2^{\cdot}$ (pKa = 4.8) which acted as the precursor of H_2O_2 as the solution pH dropped during DMP photolysis.

It was also found in Fig. 3a that, DMP degradation under UV_{254} irradiation only was slowed down by adding TBA (100 mM) and the kinetics was close to a typical pseudo-first order as commonly reported for photolysis. It suggests that both direct photolysis and H_2O_2-assissted mechanisms were involved under UV_{254} irradiation. Although NO_2^- could slow down the overall degradation of DMP, it was still faster compared to that in the UV + TBA condition, which suggested that NO_2^- mainly disturbed the H_2O_2-assissted part of DMP degradation, probably by competing the O_2 and $O_2^{\cdot}$- necessary for H_2O_2 formation (reactions A12, A15-16).

The inset figure of Fig. 4a demonstrated the formation of 7-hydroxycoumarin with and without the addition of NO_x^-. It was observed that, the relative intensities of 7-hydroxycoumarin by adding NO_x^- and their formation kinetics agreed well with the degradation performance of DMP. This implied that DMP degradation related closely to the formation of $^{\cdot}$OH. Less 7-hydroxycoumarin was detected upon addition of NO_2- compared with that of NO_3-. The likely reason is that the $[NO_2\text{-}]_0$ (1 mM) was higher than $[coumarin]_0$ (0.1 mM), and NO_2- reacts faster with $^{\cdot}$OH (reaction A5) than coumarin (coumarin + $^{\cdot}$OH → products, k = 2 × 10^9 $M^{-1}s^{-1}$ [31]). Consequently, NO_2- would successfully compete for $^{\cdot}$OH with coumarin. It was interesting to observe that, the presence of NO_2^- slowed down the overall degradation rate of DMP (Fig. 3a), but higher intensity of 7-hydroxycoumarin was detected compared to sole-UV condition (Fig. 4a). It was likely because that, on the one hand, the quenching role of NO_2^- was more pronounced with minor concentration of organic media (DMP only in Fig. 3a), while the radical providing role turned dominant with increased amount of organics (additional coumarin in Fig. 4a); on the other hand, the decomposition of H_2O_2 should be significantly hindered by coumarin due to the "inner filter" effect ($\varepsilon_{254,\ coumarin}$ = 4070 $M^{-1}cm^{-1}$, $\varepsilon_{254,\ H2O2}$ = 18.65 $M^{-1}cm^{-1}$) and the detected $^{\cdot}$OH by coumarin was lower than the actual amount formed in Fig. 3a.

3.3.2. 300 nm UV condition

The signal of DMPO-$^{\cdot}$OH was also obtained at λ = 300 nm in the presence of NO_x^- (Fig. 4b). When DMPO concentration was overwhelming (70 mM) compared with that of NO_x^- (1 mM), the DMPO-$^{\cdot}$OH signal was much stronger with the addition of NO_2^-, indicating a higher yield of $^{\cdot}$OH. This finding suggests that in the presence of effective $^{\cdot}$OH trapping agent (e.g., DMPO or other scavengers), NO_2^- could be conserved to conduct the photosensitizing reaction.

Since photolysis of NO_2^- also included another parallel pathway, i.e., the formation of $NO_2^{\cdot}$ and a hydrated electron (reaction A10) [32] that further combined with O_2 to form $O_2^{\cdot -}$ (reaction A11) [31]. Besides, reaction of aromatics with $^{\cdot}$OH can also produce $O_2^{\cdot -}$ (D1, D2, B3). The ESR technique was also applied for $O_2^{\cdot -}$ detection. As shown in Fig. 4c, four characteristic peaks were observed for the DMPO-$^{\cdot}O_2^-$ signal with the addition of either NO_2^- or NO_3^- as the triggering species, confirming the occurrence of $O_2^{\cdot -}$. The intensity of the DMPO-$^{\cdot}O_2^-$ signal was higher with NO_2^- as the trigger, most likely because that the NO_2^- as the photoconversion product of NO_3^- should be accumulated before it could produce comparative $O_2^{\cdot -}$.

3.3.3. Competitive tests using radical quenchers

To elucidate the dominant radical species contributing to DMP decomposition, TBA (100 mM) was applied as the ˙OH scavenger. Fig. S8 shows the DMP removal rate at different conditions. At λ = 300 nm or 350 nm, the addition of TBA in the presence of NO_x^- decreased DMP degradation significantly to a rate similar to that under UV-only irradiation. At λ = 254 nm, TBA could even slow down DMP photolysis, and the 4 h removal rate decreased from 79.6% to 45%, suggesting the important role of ˙OH during direct photolysis. All of the above results with TBA addition demonstrated well that ˙OH was the dominant ROS responsible for improving DMP degradation in the presence of NO_x^-. Since $^{\cdot}O_2^-$ has moderate oxidizing power (i.e., E^0 ($HO_2^{\cdot}/H_2O_2$) = 1.44 V_{NHE} or E^0 ($O_2^{\cdot -}/HO_2^-$) = 1.03 V_{NHE}) [10], it is possible to use it for oxidizing some metal ions or very labile organic compounds. Meanwhile Liu et al. [33] showed that superoxide radicals are incapable of degrading DMP, which is consistent with the results of the present study that ˙OH was the main contributor in the oxidation.

3.4. Quantitative analysis of ˙OH produced by NO_x^-

Although both nitrites and nitrates can serve as photosensitizers to provide ROS, the role of NO_2^- in catalyzing DMP photodegradation was more complicated as discussed above. Additionally, NO_2^- is assumed to be a reduction product for the photolysis of NO_3^- (reactions C2, C3, A8, A9), resulting in the coexistence of NO_3^- and NO_2^-. Therefore, experiments were designed at λ = 300 nm to elucidate the influence of photoconversion of NO_2^-/NO_3^- on DMP degradation.

Fig. 5 shows the formation of 7-hydroxycoumarin ([coumarin]$_0$ = 1 mM) during the photolysis of NO_x^-, and single NO_x^- (NO_3^- or NO_2^-) was applied as the trigger at two different concentrations (0.05 mM and 1 mM). For all of the studied conditions, DMP degradation was completely inhibited (data not shown), implying the complete scavenging of ˙OH. Meanwhile, coumarin exhibited strong light absorption ($\varepsilon_{coumarin,300}$ = 6120 $M^{-1}\,cm^{-1}$), strengthening the "inner filter" effect, and the direct photolysis of DMP was also suppressed. As a consequence, the presence of trace DMP was found to have no observable influence on 7-hydroxycoumarin formation, confirming the depletion of produced ˙OH. It was clearly observed from Fig. 5 that, generally, 7-hydroxycoumarin was produced faster when NO_2^- was applied as the trigger. At low [NO_x^-]$_0$ (0.05 mM), the initial production rate was *ca.* 3.6 times higher for NO_2^- than for NO_3^-, which was close to the proportional relation of the corresponding quantum yields ($\Phi_{nitrite308}$: $\Phi_{nitrate308}$ = 6.9% : 1.7% ≈ 4) [1]. It follows that, the self-quenching role of NO_2^- can be sufficiently suppressed in the presence of excess exogenous ˙OH acceptors, in accordance with the results observed from ESR signal (Fig. 4b). However, when [NO_x^-]$_0$ increased 20-fold to 1 mM and was equal to [coumarin]$_0$, the production of 7-hydroxycoumarin only increased moderately. Stronger competition for ˙OH induced by NO_2^- and other photolysis products of NO_x^- was assumed to be the cause of this effect. On the other hand, the strong "inner filter" effect most likely hindered NO_x^- photolysis.

3.5. Conversion of NO_2^-/NO_3^- in catalyzing low concentration DMP

Since photolysis of NO_x^- produces nitrogen oxide radicals (NO˙ or $NO_2^{\cdot}$), they can rapidly recombine to regenerate NO_2^- or NO_3^- (reaction A6-A9). Variation of [NO_x^-] during the photoconversion with and without the presence of DMP was monitored at 300 nm (Fig. 6). Generally, the generation of NO_2^- during NO_3^- photolysis (Fig. 6a) was found to be slower than NO_3^- formation induced by NO_2^- photolysis (Fig. 6b). This implied that the $NO_2^- \rightarrow NO_3^-$ conversion proceeded more easily than that of $NO_3^- \rightarrow NO_2^-$, but this faster conversion did not lead to an accompanying higher removal rate of DMP (Fig. 2). These results provided a good confirmation for the self-quenching reaction between NO_2^- and ˙OH because the formation of

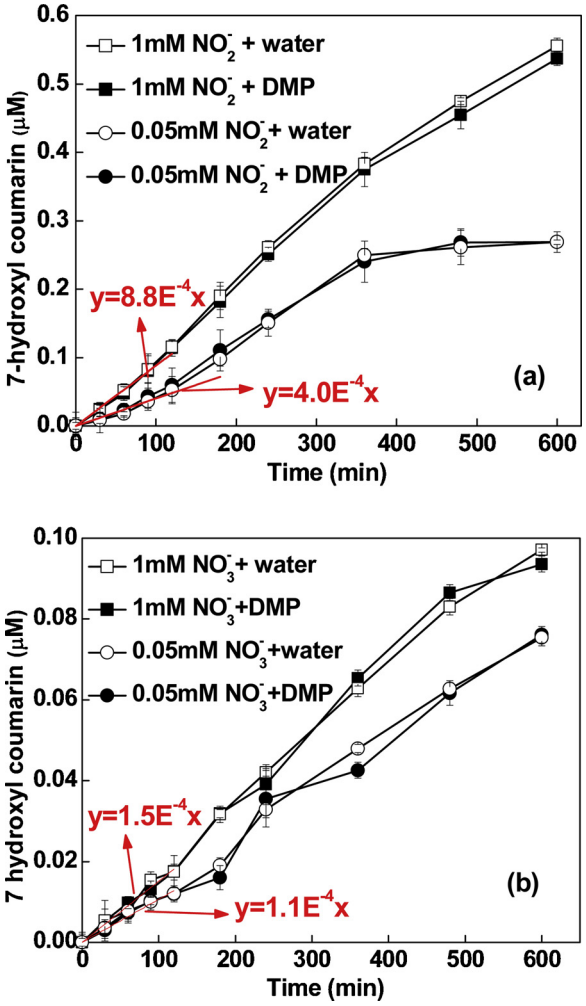

Fig. 5. Production of 7-hydroxycoumarin (coumarin-˙OH adduct) during photolysis of NO_x^- with and without the presence of DMP (conditions: [coumarin]$_0$ = 1 mM, [DMP]$_0$ = 0.01 mM, [NO_x^-]$_0$ = 0.05 mM or 1 mM, 300 nm UV).

NO_3^- (reaction A9) is mainly due to the dimerization of $NO_2^{\cdot}$ (reactions A8 and A9), which is the reaction product between NO_2^- and ˙OH (reaction A5). It was also observed that the presence of DMP facilitated the conversions of $NO_2^- \rightarrow NO_3^-$ and $NO_3^- \rightarrow NO_2^-$, similar to the results obtained in metal-ion-mediated conditions [10]. Most likely, this was because the consumption of ˙OH by DMP hindered the recombination of $NO_2^{\cdot}$ and ˙OH (reactions C4 and C5), and NO˙ and $O^{\cdot -}$, favoring further transformation from NO_2^- to NO_3^- (or NO_3^- to NO_2^-). In the process of the mutual transformation between NO_2- and NO_3, the concurrent decrease of precursor NO_3^- (or NO_2^-) was found to be stoichiometrically higher than the production of NO_2^- (or NO_3^-), which was more pronounced when NO_3^- was used as the precursor. Fig. S9 shows the sum of NO_2^- and NO_3^- concentrations in solution, and also the corresponding decrease of TN in solution implying the amount of nitrogen migrating into the gas phase. Generally, the presence of DMP resulted in more TN loss compared to pure water system, in accordance with the findings of Laurentiis et al. (2015) that the production of gas-phase nitrogen was enhanced by the presence of ˙OH scavengers upon nitrite irradiation [34]. By comparison, the minor imbalance may be related to the nitration phenomenon of background organics (e.g., DMP and its intermediates).

In view of the coexistence of NO_2^- and NO_3^- during the photoconversion of NO_x^-, mixtures of NO_2^- and NO_3^- in varying proportions (total amount = 1 mM) were applied at the beginning to examine

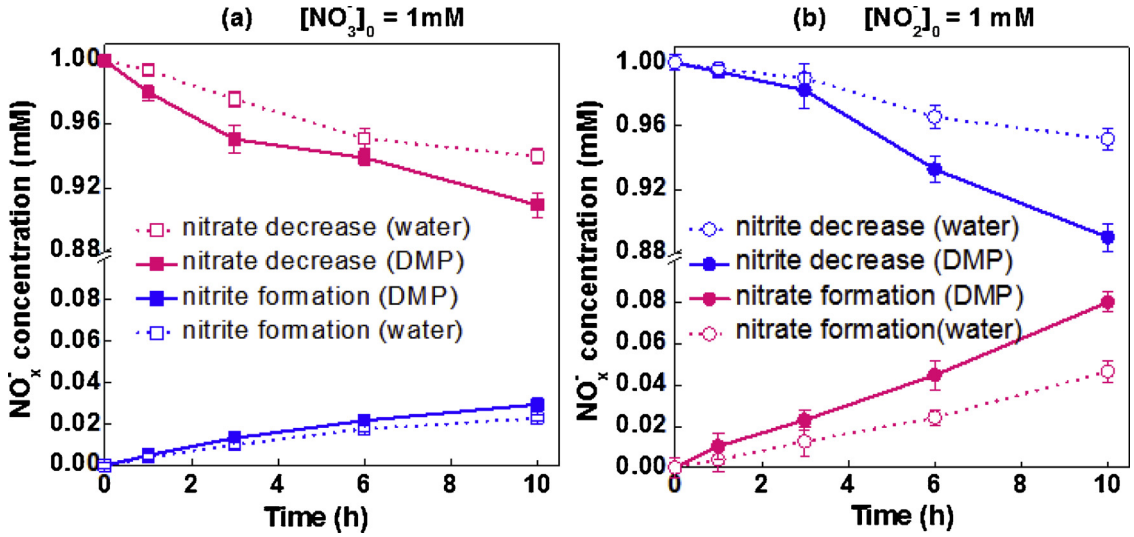

Fig. 6. Conversion between NO_2^- and NO_3^- under UV light irradiation at 300 nm UV light with and without the presence of DMP (conditions: $[DMP]_0$ = 0.01 mM, $[NO_2^-]_0$ or $[NO_3^-]_0$ = 1 mM, pH_0 = 6.2 ± 0.2).

the influence. As shown in Fig. S10, it was found that the relative proportions of NO_2^- and NO_3^- did not make a significant difference for DMP degradation at low concentration (0.01 mM) only if NO_2^- was involved as the precursor; this was ascribed to the strong scavenging of the produced ˙OH by NO_2^-. As noted in Fig. 2(b) and S10, the DMP degradation kinetics showed gradual deceleration during each reaction when using NO_3^- as the initial trigger. This may be due to the gradual photoreduction of NO_3^- to NO_2^- (Fig. 6a) increasing the radical competition between DMP and NO_2^-. A similar phenomenon was also clearly observed for irradiation at 254 nm (Fig. 3b). Although DMP degradation was enhanced by nitrate catalysis, the improvement was more significant in the initial period. These results suggested that for treating relatively low concentrations of DMP, NO_3^- was more effective than NO_2^-.

3.6. Conversion of NO_2^-/NO_3^- in catalyzing high concentration DMP

3.6.1. 350 nm UV condition

Since it was found that the radical scavenging effect of NO_2^- can be inhibited in the presence of high organic content, DMP at high concentration ($[DMP]_0$:$[NO_x^-]_0$ = 2 or 4) was applied to examine the role of NO_x^-. Fig. 7a and b show the variation of the DMP removal (in mM) and the accompanying NO_2-→NO_3- conversion at λ = 350 nm, respectively. Since DMP was completely inert at 350 nm, its degradation was almost entirely due to radical reactions. Fig. 7b shows the complete disappearance of NO_2- with approximately 85% of NO_2- converted to NO_3- based on stoichiometrical calculation. TN loss in solution was also detected in the later phase of reaction (> 8 h, see Fig. S11), and therefore nitration of DMP may be nonsignificant in view of the low level nitrogen dosing (0.1 mM). Due to the unresponsiveness of NO_3-, cycling between NO_3- and NO_2- is unlikely to occur for irradiation at λ = 350 nm. Interestingly, the variation of DMP removal shown in Fig. 7a was found to be in good agreement with the decrease of NO_2-; as NO_2- reached its full conversion, DMP removal also showed saturation. Fig. S12 shows Δ[NO_2-]:Δ[DMP] during the reaction, where it was observed that the ratio remained almost constant and was close to 1 (r_{avg} = 0.93 for $[DMP]_0$ = 0.4 mM, r_{avg} = 1.05 for $[DMP]_0$ = 0.2 mM) during the catalytic process. Since TOC was also decreased by 10.2% and 5.7% for 0.2 mM and 0.4 mM DMP, respectively (data not shown), the Δ[NO_2-]:Δ[˙OH] ratio should be < < 1. The fact that Δ[NO_2-]:Δ[˙OH] < < 1 implied that NO_2- should be regenerated to continuously supply ˙OH radicals when these radicals are captured by abundant DMP and/or the intermediates. NO_2- was most likely regenerated via the combination of NO˙ and NO_2˙ (reactions A6 and A7) that should occur more easily, as ˙OH was eliminated by DMP. Since formation of NO_3- would terminate the photosensitizing reaction, it can be inferred that regeneration of NO_2- occurs more easily than formation of NO_3- (reactions A8 and A9) to produce significant DMP decomposition and mineralization. The pathway for the direct production of NO_2˙ by excited state NO_2^- (reaction A10) was supposed to be of minor importance [10], and even inconclusive [1], so that it is likely that the available NO_2˙ was converted from the oxidation of NO˙ (reactions A12 and A13).

3.6.2. 300 nm UV condition

Experiments were also carried out for irradiation at λ = 300 nm (Fig. 7c, d). It was found that both NO_3^- and NO_2^- significantly improved DMP degradation so that complete degradation was achieved, even though $[NO_x^-]_0$ < $[DMP]_0$ ($[NO_x^-]_0$:$[DMP]_0$ = 1:2). NO_2^- was found to be more efficient in accelerating DMP degradation (Fig. 7c) and the accompanying complete conversion of NO_2^-→NO_3^- is also observed in Fig. 7d. However, using NO_3^- as the trigger, it was found that the concentrations of both NO_3^- and NO_2^- remained almost constant during the entire reaction. Considering the fast decomposition of DMP, it was inferred that NO_2^- was immediately converted back to NO_3^- as soon as it was formed, i.e., the reaction involved fast cycling between NO_3^- and NO_2^-. It was also found that DMP degradation showed a clear lag phase (ca. 6 h) when applying NO_3^-. This may be because NO_2^- that has a higher photolysis quantum yield is to be accumulated to a certain degree before it can give rise to significant acceleration. Additionally, as the degradation process advanced, the solution pH gradually decreased, and the nitrous acid (HNO_2, pKa = 3.2) with a high quantum yield for ˙OH generation (reaction A14, $\Phi_{OH,300}$ = 36.2 ± 4.7%) [32] increased to improve DMP degradation. The evolution profiles of TOC (Fig. 7c) showed similar trends, which demonstrated the best mineralization performance (40.2%) in the UV/NO_2^- process and a lag phase (ca. 12 h) in the UV/NO_3^- process. When NO_2^- was completely converted to NO_3^-, TOC decrease and DMP degradation could still proceed due to the action of irradiated NO_3^-.

3.7. DMP degradation pathways

The possible degradation intermediates were identified to further interpret the mechanism for DMP degradation. Table S1 summarizes the detailed information of the identified intermediates in the UV/NO_3^- and UV/NO_2^- processes at λ = 300 nm (same conditions as for the results shown in Fig. 7c). Generally, the same species of

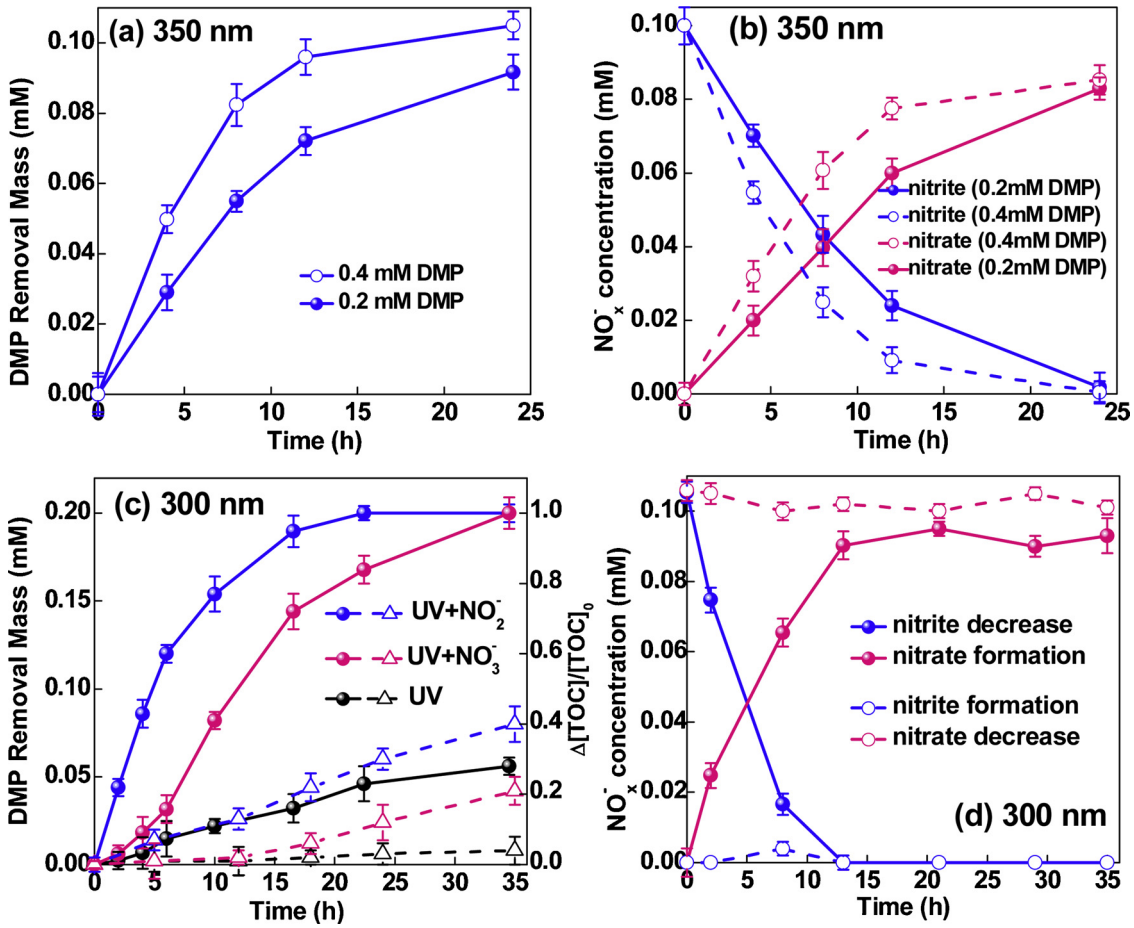

Fig. 7. (a) DMP removal molarity at different DMP concentrations ($[DMP]_0$ = 0.2 or 0.4 mM) at λ = 350 nm, (b) photochemical conversion of NO_2^- to NO_3^- at different DMP concentrations ($[DMP]_0$ = 0.2 or 0.4 mM) at λ = 350 nm, (c) DMP removal molarity at λ = 300 nm (solid points) and TOC variation (hollow points) ($[DMP]_0$ = 0.2 mM), (d) photochemical conversion of NO_2^- to NO_3^- at λ = 300 nm ($[DMP]_0$ = 0.2 mM), (conditions: $[NO_x^-]_0$ = 0.1 mM, pH_0 = 6.2 ± 0.2).

intermediates were identified but with different variation profiles, suggesting that similar mechanisms were involved in both UV/NO_3^- and UV/NO_2^- systems due to the continuous cycling between NO_3^- and NO_2^-.

Based on the identified intermediates, it was concluded that DMP degradation was mainly induced by three different mechanisms as shown in Fig. 8, namely ˙OH addition to the aromatic ring (mono-, dihydroxylated DMP), hydrogen atom abstraction by ˙OH (aliphatic chain derivatives), and nitration of the aromatic ring. An et al. (2013) also reported the first two pathways as the dominant reaction processes for DMP degradation in ˙OH-mediated AOTs [35]. The variation profiles of mass peak area of both DMP and the primary intermediates are provided in Table S1. As the DMP amount decreased, a majority of the primary products concurrently experienced an accumulation period and a subsequent decrease, indicating that degradation of DMP and the primary products proceeded simultaneously. Some of the primary intermediates also completely disappeared when DMP was entirely removed. It was also seen that for most intermediates shown in Table S1, the maximum concentration and the disappearance were obtained earlier in the UV/NO_2^- process than that in the UV/NO_3^- process, in good agreement with the results discussed above regarding the higher effectiveness of NO_2^- for providing ˙OH. Only one ring opening product was detected in the present study (No. 10), which was also reported by Chen et al. [36], and its maximum concentration was achieved much more slowly than those for the aromatic intermediates, suggesting that the ring opening products were the secondary products prior to mineralization.

These results of the intermediates analysis agree with the better mineralization performance (Fig. 7c) of the UV/NO_2^- process. In addition, two nitration products with relatively weak signals were detected in this study (Nos. 1 and 6), suggesting that nitration was not the dominant pathway for DMP degradation even though $NO_2^{\cdot}$ has been reported to be involved in the nitration of many aromatic compounds, such as phenol [37]. Since most nitration products were reported to be more toxic, the scarcity of nitration products has advantageous environmental implications for the application of the NO_3^-/NO_2^- photocatalytic processes.

3.8. Implications for wastewater treatment

Coupling the indigenous NO_3^- or NO_2^- in wastewater effluent with proper light conditions (sunlight or UV light) can create an advanced oxidation environment to further degrade the residue recalcitrant organic contaminants. One of the promising aspects is that the cycling between NO_3^- and NO_2^- can be promoted by the presence of organic pollutants, and the radical scavenging role of NO_2^- can also be inhibited by the presence of sufficient organic pollutants. For those emerging contaminants showing photoinert properties, this approach provides a feasible way to control their release to the natural environment. Particularly, the UV/NO_x^- process has the advantage over UV/H_2O_2 when using sunlight as the light source due to the stronger light absorption of NO_3^- and NO_2^- at λ > 300 nm (see Fig. S4). Since effluent organic matters (EfOM) existing in the effluent, particularly the natural organic matters (NOM), also show photoactivity, interactions between EfOM and NO_x^- need to be clarified in further studies.

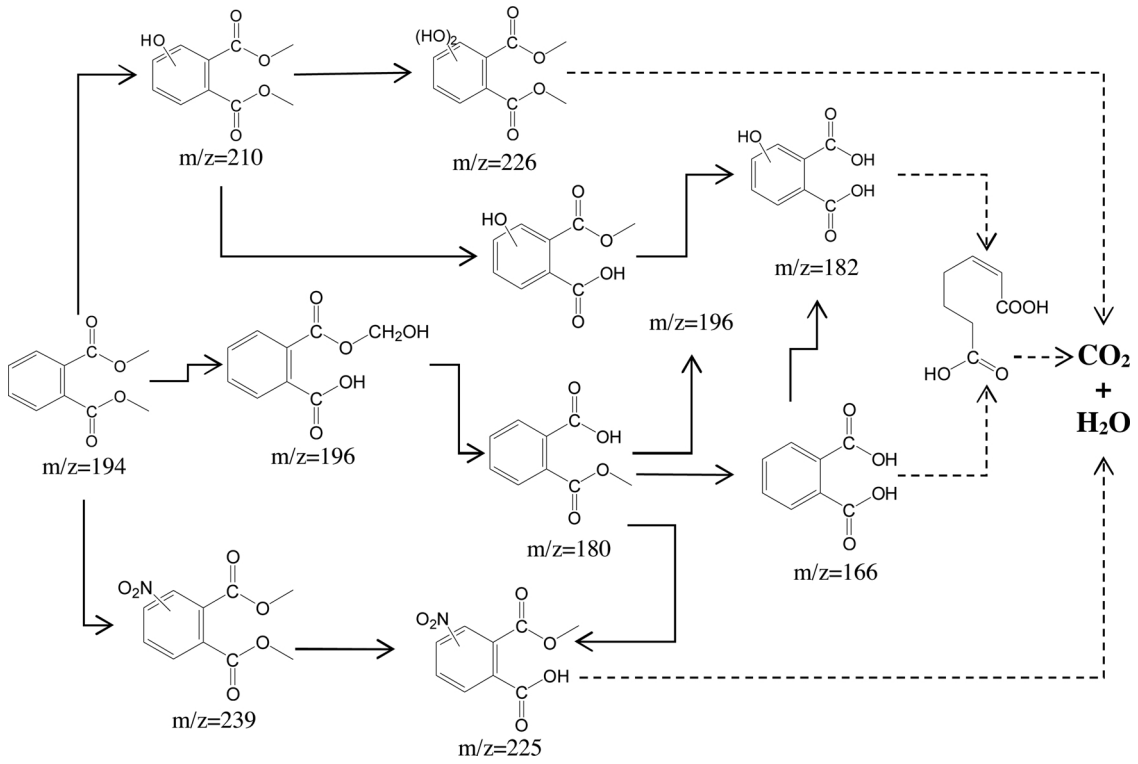

Fig. 8. Proposed pathways of DMP degradation in different processes based on LCMS analysis ($[DMP]_0$ = 0.2 mM, $[NO_x^-]_0$ = 0.1 mM).

4. Conclusions

This study showed that the photoconversion of NO_3^- or NO_2^- can serve as an advanced oxidation process for mineralizing DMP. The influence of NO_3^- or NO_2^- was found to be wavelength-dependent, and also relied on the relative proportion between NO_x^- and effective ·OH trapping agent. Hydroxyl radicals were the dominant ROS for DMP degradation. NO_3- was more efficient for treating low-level DMP, while NO_2- was capable to catalyze DMP degradation at high concentrations. At λ = 300 nm, continuous cycling between NO_2- and NO_3- enabled the complete degradation of DMP at concentrations higher than those of NO_x^-. For irradiation at λ = 350 nm, NO_3- was completely ineffective and self regeneration of NO_2- enabled the amount of ·OH produced to be higher than the steady-state decrease of NO_2-. The hydrogen atom abstraction by ·OH and ·OH addition to the aromatic ring were the dominant pathways. Nitration products were detected but at low levels.

Declaration of Competing Interest

The authors declare that they have no known competing financial interests or personal relationships that could have appeared to influence the work reported in this paper.

Acknowledgements

This study was financially supported by the National Natural Science Foundation of China (No. 51708297), the Natural Science Foundation of Jiangsu Province (No. BK20160936, No. BK20160938, No. BK20160930), the Priority Academic Program Development of Jiangsu Higher Education Institutions (PAPD) and the Postgraduate Research & Practice Innovation Program of Jiangsu Province (KYCX19_1112). The advanced analysis and testing center of Nanjing Forestry University is also acknowledged.

Appendix A. Supplementary data

Supplementary material related to this article can be found, in the online version, at doi:https://doi.org/10.1016/j.apcatb.2019.117958.

References

[1] J. Mack, J.R. Bolton, Photochemistry of nitrite and nitrate in aqueous solution: a review, J. Photochem. Photobiol. A Chem. 128 (1999) 13.
[2] D. Vione, M. Minella, V. Maurino, C. Minero, Indirect photochemistry in sunlit surface waters: photoinduced production of reactive transient species, Chem. Eur. J. 20 (2014) 10590–10606.
[3] D. Vione, C. Minero, V. Maurino, E. Pelizzetti, Seasonal and water column trends of the relative role of nitrate and nitrite as (OH)-O-center dot sources in surface waters, Ann. Chim. 97 (2007) 699–711.
[4] Hanbo Yu, Binbin Huang, Hou Wang, Xingzhong Yuan, Longbo Jiang, Zhibin Wu, Jin Zhang, G. Zeng, Facile construction of novel direct solid-state Z-scheme AgI/BiOBr photocatalysts for highly effective removal of ciprofloxacin under visible light exposure: mineralization efficiency and mechanisms, J. Colloid Interface Sci. 522 (2018) 82–94.
[5] H. Yu, L. Jiang, H. Wang, B. Huang, X. Yuan, J. Huang, J. Zhang, G. Zeng, Modulation of Bi2 MoO6 -Based Materials for Photocatalytic Water Splitting and Environmental Application: a Critical Review, Small (Weinheim an der Bergstrasse, Germany), (2019) e1901008–e1901008.
[6] M. Chen, J. Yao, Y. Huang, H. Gong, W. Chu, Enhanced photocatalytic degradation of ciprofloxacin over Bi_2O_3/$(BiO)_2CO_3$ heterojunctions: efficiency, kinetics, pathways, mechanisms and toxicity evaluation, Chem. Eng. J. 334 (2018) 453–461.
[7] M. Chen, W. Chu, H_2O_2 assisted degradation of antibiotic norfloxacin over simulated solar light mediated Bi2WO6: kinetics and reaction pathway, Chem. Eng. J. 296 (2016) 310–318.
[8] Longbo Jiang, Xingzhong Yuan, Guangming Zeng, Jie Liang, Zhibin Wu, Hou Wang, Jin Zhang, Ting Xiong, H. Li, A facile band alignment of polymeric carbon nitride isotype heterojunctions for enhanced photocatalytic tetracycline degradation, Environ. Sci. Nano 5 (2018) 2604–2617.
[9] M.V. Shankar, S. Nelieu, L. Kerhoas, J. Einhorn, Natural sunlight NO_3-/NO_2—Induced photo-degradation of phenylurea herbicides in water, Chemosphere 71 (2008) 1461–1468.
[10] D.-h. Kim, J. Lee, J. Ryu, K. Kim, W. Choi, Arsenite oxidation initiated by the UV photolysis of nitrite and nitrate, Environ. Sci. Technol. 48 (2014) 4030–4037.
[11] C.M. Sharpless, D.A. Seibold, K.G. Linden, Nitrate photosensitized degradation of atrazine during UV water treatment, Aquat. Sci. 65 (2003) 359–366.
[12] G.-L. Liu, L. Gong, L. Hu, D.-W. Zhu, X.-Y. Cao, C.-L. Song, Y.-Y. Zhou, NO_3-/NO_2-photosensitized degradation of phenol under simulated sunlight, Fresenius Environ. Bull. 24 (2015) 664–669.
[13] P. Calza, D. Vione, A. Novelli, E. Pelizzetti, C. Minero, The role of nitrite and nitrate

ions as photosensitizers in the phototransformation of phenolic compounds in seawater, Sci. Total Environ. 439 (2012) 67–75.
[14] S. Nelieu, L. Kerhoas, M. Sarakha, J. Einhorn, Nitrite and nitrate induced photodegradation of monolinuron in aqueous solution, Environ. Chem. Lett. 2 (2004) 83–87.
[15] M.V. Shankar, S. Nelieu, L. Kerhoas, J. Einhorn, Photo-induced degradation of diuron in aqueous solution by nitrites and nitrates: kinetics and pathways, Chemosphere 66 (2007) 767–774.
[16] L.J. Xu, W. Chu, P.-H. Lee, J. Wang, The mechanism study of efficient degradation of hydrophobic nonylphenol in solution by a chemical-free technology of sonophotolysis, J. Hazard. Mater. 308 (2016) 386–393.
[17] L.E. Jacobs, L.K. Weavers, E.F. Houtz, Y.-P. Chin, Photosensitized degradation of caffeine: role of fulvic acids and nitrate, Chemosphere 86 (2012) 124–129.
[18] S. Bahnmueller, U. von Gunten, S. Canonica, Sunlight-induced transformation of sulfadiazine and sulfamethoxazole in surface waters and wastewater effluents, Water Res. 57 (2014) 183–192.
[19] C. Zhou, J. Chen, Q. Xie, X. Wei, Y.-n. Zhang, Z. Fu, Photolysis of three antiviral drugs acyclovir, zidovudine and lamivudine in surface freshwater and seawater, Chemosphere 138 (2015) 792–797.
[20] O.S. Keen, N.G. Love, K.G. Linden, The role of effluent nitrate in trace organic chemical oxidation during UV disinfection, Water Res. 46 (2012) 5224–5234.
[21] https://toxnet.nlm.nih.gov/.
[22] G. Hizal, Q.Q. Zhu, C.-H. Fischer, P.M. Fritz, W. Schnabel, On the photolysis of phthalic acid dialkyl esters: a product analysis study, J. Photochem. Photobiol. A Chem. 72 (1993) 147–152.
[23] D.W. O'Sullivan, M. Tyree, The kinetics of complex formation between Ti(IV) and hydrogen peroxide, Int. J. Chem. Kinet. 39 (2007) 457–461.
[24] J. Zhang, Y. Nosaka, Quantitative detection of OH radicals for investigating the reaction mechanism of various visible-light TiO_2 photocatalysts in aqueous suspension, J. Phys. Chem. C 117 (2013) 1383–1391.
[25] L.S. Clesceri, A.E. Greenberg, A.D.E (Eds.), Standard Methods for the Examination of Water and Wastewater, 20th ed., American Public Health Association (APHA), Washington, DC, 1998.
[26] L.J. Xu, W. Chu, N. Graham, Sonophotolytic degradation of phthalate acid esters in water and wastewater: influence of compound properties and degradation mechanisms, J. Hazard. Mater. 288 (2015) 43–50.
[27] P. Warneck, C. Wurzinger, Product quantum yields for the 305-nm photodecomposition of NO_3- in aqueous solution, J. Phys. Chem. 92 (1988) 6278–6283.
[28] G. Wen, J. Ma, Z.-Q. Liu, L. Zhao, Ozonation kinetics for the degradation of phthalate esters in water and the reduction of toxicity in the process of O-3/H_2O_2, J. Hazard. Mater. 195 (2011) 371–377.
[29] J. Ryu, D. Monllor-Satoca, D.-h. Kim, J. Yeo, W. Choi, Photooxidation of arsenite under 254 nm irradiation with a quantum yield higher than unity, Environ. Sci. Technol. 47 (2013) 9381–9387.
[30] B.H.J. Bielski, D.E. Cabelli, R.L. Arudi, Reactivity of $H0_2/0_2$ radicals in aqueous solution, J. Phys. Chem. Ref. Data 14 (1985) 1041–1100.
[31] G.V. Buxton, C.L. Greenstock, W.P. Helman, A.B. Ross, Critical review of rate constants for reactions of hydrated electrons, hydrogen atoms and hydroxyl radicals (.OH/O-) in aqueous solution, J. Phys. Chem. Ref. Data 17 (1988) 513–886.
[32] M. Fischer, P. Warneck, Photodecomposition of nitrite and undissociated nitrous acid in aqueous solution, J. Phys. Chem. 100 (1996) 18749–18756.
[33] Y. Liu, D. Wu, S. Peng, Y. Feng, Z. Liu, Enhanced mineralization of dimethyl phthalate by heterogeneous ozonation over nanostructured Cu-Fe-O surfaces: Synergistic effect and radical chain reactions, Sep. Purif. Technol. 209 (2019) 588–597.
[34] E. De Laurentiis, M. Minella, S. Berto, V. Maurino, C. Minero, D. Vione, The fate of nitrogen upon nitrite irradiation: formation of dissolved vs. gas-phase species, J. Photochem. Photobiol. A Chem. 307 (2015) 30–34.
[35] T. An, Y. Gao, G. Li, P.V. Kamat, J. Peller, M.V. Joyce, Kinetics and mechanism of (OH)-O-center dot mediated degradation of dimethyl phthalate in aqueous solution: experimental and theoretical studies, Environ. Sci. Technol. 48 (2014) 641–648.
[36] Y.-H. Chen, L.-L. Chen, N.-C. Shang, Photocatalytic degradation of dimethyl phthalate in an aqueous solution with Pt-doped TiO_2-coated magnetic PMMA microspheres, J. Hazard. Mater. 172 (2009) 20–29.
[37] D. Vione, V. Maurino, C. Minero, E. Pelizzetti, New processes in the environmental chemistry of nitrite: nitration of phenol upon nitrite photoinduced oxidation, Environ. Sci. Technol. 36 (2002) 669–676.